Modified LAMBDA for absolute carrier phase positioning in the presence of biases

P. Henkel*, V. Gomez* and C. Günther*,**
*Technische Universität München (TUM), Munich, Germany
**German Aerospace Center (DLR), Oberpfaffenhofen, Germany

BIOGRAPHIES

Patrick Henkel studied electrical engineering and information technology at the Technische Universität München (TUM), Germany and the École Polytechnique de Montréal, Canada. He is a PhD student at the Institute of Communications and Navigation at TUM since 2005 and focuses on robust ambiguity resolution for precise carrier phase positioning with multiple frequencies. In 2007, he was a guest researcher at TU Delft and won the Pierre Contensou Gold medal at the International Astronautical Congress. In 2008, he received a DAAD fellowship for a research visit of the GPS lab at Stanford University where he worked on wideband ionospheric corrections for multi-carrier, multi-satellite vector phase locked loops.

Víctor Gómez has received an Ing. degree in electrical and communications engineering from the Universidad Tecnológica de México, Mexico, in 2003. He has then worked for two years as a field test engineer in the mobile devices division of Motorola. Since 2006, he is a M.Sc. student in electrical engineering at the Technische Universität München, Germany, and is currently working on his thesis on partial ambiguity fixing in the presence of biases.

Christoph Günther studied theoretical physics at the Swiss Federal Institute of Technology in Zurich. He received his diploma in 1979 and completed his PhD in 1984. He worked on communication and information theory at Brown Boveri and Ascom Tech. From 1995, he led the development of mobile phones for GSM and later dual mode GSM/Satellite phones at Ascom. In 1999, he became head of the research department of Ericsson in Nuremberg. Since 2003, he is the director of the Institute of Communication and Navigation at the German Aerospace Center (DLR) and since December 2004, he additionally holds a Chair at the Technische Universität München (TUM). His research interests are in satellite navigation, communication, and signal processing.

ABSTRACT

The least-squares integer ambiguity decorrelation adjustment (LAMBDA) method is adapted for absolute positioning with satellite-satellite single difference measurements. The integer decorrelation transformation of LAMBDA takes only the covariance matrix of float ambiguities into account which results in a substantial amplification of biases due to orbital errors, satellite clock offsets and multipath. Therefore, a partial integer decorrelation is suggested to achieve the optimum trade-off between variance reduction and bias amplification. The reliability of ambiguity resolution is further improved by using two geometry-preserving, ionosphere-free multi-frequency linear combinations: a code-carrier combination of maximum discrimination and a code-only combination of minimum noise. The optimized widelane and narrowlane linear combinations are presented for two, three and four Galileo frequencies. The achievable probabilities of wrong fixing have been computed for an exponential bias profile and are several orders of magnitude lower than in the case of complete integer decorrelation. Moreover, a partial fixing scheme is proposed for severe carrier phase multipath. The method bounds the biases by an exponential profile and determines the optimum fixing order by a sequential search with an azimuthal separation constraint between the satellites of two consecutive ambiguity fixings.

INTRODUCTION

Carrier phase measurements are extremely precise but ambiguous. If double difference measurements are computed for baselines up to 100 km, the ambiguities can be considered integer valued due to the substantial suppression of errors in the orbits and satellite clocks. The Least-Square Ambiguity Decorrelation Adjustment (LAMBDA) method has been proposed by Teunissen in [1] to find the integer least-square solution. It starts with a real-valued least-square estimation of the ambiguities and consists of

three steps: First, an integer decorrelation transformation is computed from the covariance matrix of float ambiguities to reduce the search space. This volume preserving transformation is obtained by Jonge and Tiberius in [2] from alternating integer approximated Gaussian eliminations and permutations of ambiguities. Both the transformation and its inverse are integer valued to preserve the integer nature during the back-transformation after fixing. Secondly, a search is performed to find the integer ambiguities that minimize the integer least-square error norm of decorrelated ambiguities. Finally, the fixed ambiguities are transformed into the original ambiguity space using the inverse of the decorrelation matrix. Several test criteria have been suggested for integer validation, e.g. the ratio test by Euler and Schaffrin in [3] which discriminates between the integer estimates of lowest and second lowest error norms. The integer decorrelation transformation can also be used for any other fixing method, e.g. the widely used bootstrapping. However, LAMBDA achieves a higher success rate than bootstrapping as long as no biases are present.

For absolute positioning with satellite-satellite single difference measurements, LAMBDA does not achieve the integer least-square solution as the integer decorrelation transformation amplifies residual biases (due to orbital errors, satellite clock errors and carrier phase multipath) which partially compensate the gain obtained from the variance reduction. Therefore, a partial integer decorrelation is suggested to obtain an optimum trade-off between variance reduction and bias amplification for absolute carrier phase positioning. For a wide range of phase and code biases, the probabilities of wrong fixing are several orders of magnitude lower than in the case of a complete integer decorrelation. The partial integer decorrelation is implemented by a reduced number of alternating decorrelation and permutation steps which also makes it beneficial with respect to complexity. The number of required decorrelation steps decreases rather fast with increasing biases and converges to a single iteration for phase biases of less than 0.05 cycles.

The reliability of integer ambiguity resolution is further improved by using geometry-preserving, ionosphere-free mixed code-carrier linear combinations that maximize the ambiguity discrimination. The latter criterion has been introduced in [4] and is defined as the ratio between wavelength and standard deviation of the combination noise and is an indicator for the reliability of ambiguity resolution. A new E1-E5-E6 mixed code-carrier combination is found which is characterized by a wavelength of 4.019 m, a noise level of 5 centimeters and an E1 code multipath suppression of 17 dB. The discrimination of this combination is more than five time larger than the discrimination of the optimized dual frequency E1-E5a linear combination with a similar wavelength. The noise variance of the mixed code-carrier combination is further reduced by an ionosphere-free carrier smoothing.

All ambiguities can not be fixed with a probability of wrong fixing of 10^{-9} during severe multipath. Therefore, a new method is suggested to find the largest subset of reliably fixable ambiguities and the optimum fixing orders within the subset. An exhaustive search is simplified by constraints on the probability of wrong fixing and the azimuthal separation between two consecutive ambiguity fixings. The optimum fixing orders are shown in skyplots for an exponential bias profile.

ABSOLUTE CARRIER PHASE POSITIONING

Absolute carrier phase positioning determines the receiver position without the need of a reference station. The carrier phase measurement on frequency m at user u from satellite k at epoch i is modeled as

$$\begin{aligned}\lambda_m \phi^k_{u,m}(i) \;=\; & r^k_u(i) + \delta r^k_u(i) + c\left(\delta\tau_u(i) - \delta\tau^k(i)\right) \\ & - q^2_{1m} I^k_u(i) + T^k_u(i) + \lambda_m N^k_{u,m} \\ & + b^k_{\phi_{u,m}} + \varepsilon^k_{\phi_{u,m}}(i), \end{aligned} \quad (1)$$

with the user-satellite range $r^k_u(i)$, the projected orbital error $\delta r^k_u(i)$, the user/ satellite clock errors $\{c\delta\tau_u(i), c\delta\tau^k(i)\}$, the ionospheric delay $I^k_u(i)$ on L1, the ratio of frequencies $q_{ij} = f_i/f_j$, the tropospheric delay $T^k_u(i)$, the integer ambiguity $N^k_{u,m}$, the phase bias $b^k_{\phi_{u,m}}$ and carrier phase noise $\varepsilon^k_{\phi_{u,m}}(i)$ including multipath. A similar model is used for the code measurements:

$$\begin{aligned}\rho^k_{u,m}(i) = & \, r^k_u(i) + \delta r^k_u(i) + c\left(\delta\tau_u(i) - \delta\tau^k(i)\right) \\ & + T^k_u(i) + q^2_{1m} I^k_u(i) + b^k_{\rho_{u,m}} + \varepsilon^k_{\rho_{u,m}}(i), \end{aligned} \quad (2)$$

with the code bias $b^k_{\rho_{u,m}}$ and code noise $\varepsilon^k_{\rho_{u,m}}$. A multi-frequency ionosphere-free mixed code-carrier combination with a large wavelength is considered for absolute positioning to increase the robustness of ambiguity resolution. The linear combination is applied to satellite-satellite single differences (SD) which are not affected by the receiver clock offset. The obtained combinations for K satellites are corrected for the satellite positions, satellite clock offsets and dry components of the tropospheric delay. For simplicity, the user and time indices are omitted, and the resulting combinations are represented in matrix-vector notation, i.e.

$$\begin{bmatrix} \Delta\phi^{(1)}_c \\ \Delta\phi^{(2)}_c \\ \vdots \\ \Delta\phi^{(K-1)}_c \end{bmatrix} = \boldsymbol{X} \cdot \begin{bmatrix} \boldsymbol{x} \\ T_z \\ \boldsymbol{N} \end{bmatrix} + \begin{bmatrix} \varepsilon^{(1)} \\ \varepsilon^{(2)} \\ \vdots \\ \varepsilon^{(K-1)} \end{bmatrix}, \quad (3)$$

with the SD operator Δ, the receiver position $\boldsymbol{x}$, the tropospheric zenith delay T_z, the combined integer ambiguities $\boldsymbol{N}$, the noise $\varepsilon^{(k)}$ of satellite k, and the transformation $\boldsymbol{X}$

from range into position domain, i.e.

$$\boldsymbol{X} = \begin{bmatrix} \Delta \boldsymbol{e}^{(1),T} & \Delta m_{\mathrm{w}}^{(1)} & \lambda & & \\ \Delta \boldsymbol{e}^{(2),T} & \Delta m_{\mathrm{w}}^{(2)} & & \lambda & \\ \vdots & \vdots & & & \ddots \\ \Delta \boldsymbol{e}^{(K-1),T} & \Delta m_{\mathrm{w}}^{(K-1)} & & & \lambda \end{bmatrix}, \tag{4}$$

where $\boldsymbol{e}^{(k)}$ is the unit vector that points from the satellite to the receiver, $m_{\mathrm{w}}^{(k)}$ is the tropospheric mapping function that maps the wet component of the tropospheric zenith delay into slant direction, and λ denotes the wavelength of the multi-frequency ionosphere-free linear combination. Corrections for the orbit and satellite clock offset (e.g. of IGS) have an accuracy of only a few centimeters which results in a measurement bias that is included in the white noise, i.e.

$$\varepsilon^{(k)} \sim \mathcal{N}(b^{(k)}, \sigma^2). \tag{5}$$

The use of satellite-satellite single difference measurements is motivated by receiver independent biases $b^{(k)}$ that might be provided by a future augmentation system but can not be neglected so far. The traditional LAMBDA based integer ambiguity resolution is modified to increase the success rate in the presence of biases. First, the float solution of $\boldsymbol{x}$, T_z and $\boldsymbol{N}$ is computed by weighted least-square estimation from (3). Secondly, an integer decorrelation is applied which differs from the traditional integer decorrelation. Then, the ambiguities are fixed either by the LAMBDA search or by bootstrapping. Finally, the inverse of the modified integer decorrelation is applied to the fixed ambiguities. The measurement biases are unknown but it is assumed that they can be bounded by an exponential profile, i.e.

$$b_{\max}(\theta) = b_{\max}(0^\circ) \cdot e^{-\frac{\theta}{\zeta}}, \tag{6}$$

where θ denotes the elevation angle and ζ is the pendant factor of the bias bound.

MULTI-FREQUENCY MIXED CODE-CARRIER COMBINATIONS

A multi-frequency mixed code-carrier linear combination weights the phase measurements of (1) by $\alpha_1, \ldots, \alpha_M$ and the code measurements of (2) by $\beta_1, \ldots, \beta_M$ for M frequencies. The combination shall be geometry preserving (GP), i.e.

$$\sum_{m=1}^{M} \alpha_m + \sum_{m=1}^{M} \beta_m \stackrel{!}{=} 1, \tag{7}$$

and ionosphere-free (IF), i.e.

$$\sum_{m=1}^{M} \alpha_m \frac{f_1^2}{f_m^2} - \sum_{m=1}^{M} \beta_m \frac{f_1^2}{f_m^2} \stackrel{!}{=} 0. \tag{8}$$

The GP constraint refers also to all non-dispersive errors, i.e. there is no amplification of tropospheric delays, orbital errors and satellite clock offsets. Moreover, the integer nature of ambiguities shall be preserved (NP), i.e.

$$\sum_{m=1}^{M} \alpha_m \lambda_m N_m \stackrel{!}{=} \lambda N, \tag{9}$$

which can be rewritten as

$$\sum_{m=1}^{M} \underbrace{\frac{\alpha_m \lambda_m}{\lambda}}_{j_m \in \mathcal{Z}} N_m \stackrel{!}{=} N, \tag{10}$$

and the amount of integer numbers $\mathcal{Z}$. The remaining degrees of freedom are used to maximize the ambiguity discrimination which has been defined in [4] as

$$D = \frac{\lambda}{2\sigma_{\mathrm{n}}}, \tag{11}$$

with

$$\sigma_{\mathrm{n}} = \sqrt{\sum_{m=1}^{M} \alpha_m^2 \sigma_{\phi_m}^2 + \sum_{m=1}^{M} \beta_m^2 \sigma_{\rho_m}^2}. \tag{12}$$

The standard deviations σ_{ρ_m} are obtained from the Cramer Rao bound given by

$$\Gamma_m = \frac{c^2}{\frac{C}{N_0} \cdot \frac{\int (2\pi f)^2 |S_m(f)|^2 df}{\int |S_m(f)|^2 df}}, \tag{13}$$

with the speed of light c, the carrier to noise power ratio $\frac{C}{N_0}$, and the power spectral density $S_m(f)$ that has been derived by Betz in [5] for binary offset carrier (BOC) modulated signals. Table 1 shows the Cramer Rao bounds of the wideband Galileo signals.

Table 1 Cramer Rao Bounds for $C/N_0 = 45\mathrm{dB/Hz}$

	Signal	BW [MHz]	Γ [cm]
E1	MBOC	20	11.14
E5	AltBOC(15,10)	51	1.95
E5a	BPSK(10)	20	7.83
E5b	BPSK(10)	20	7.83
E6	BOC(10,5)	40	2.41

The metric D of (11) is used to select the linear combination that minimizes the probability of wrong fixing over all linear combinations. The optimization includes a numerical search over all integers j_m. It is sufficient to search over all $|j_m| \leq 5$ as all other combinations suffer from substantial noise and bias amplifications. Table 2 and 3 show the weighting coefficients and properties of mixed code-carrier widelane combinations of maximum discrimination with two, three and four Galileo frequencies. The dual frequency E1-E5 linear combination benefits from a wavelength of 3.285 m and a substantial suppression of the E1 code noise. It is used in the later analysis. The additional use of E6 measurements increases the ambiguity discrimination by 50 %. Table 4 refers to narrowlane combinations where the difference between two, three and four frequency combinations is negligible.

Table 2 GP-IF-NP mixed code-carrier widelane combinations of max. discrimination for $\sigma_\phi = 1\text{mm}$, $\sigma_{\rho_m} = \Gamma_m$

	E1	E5a	E5b	E5	E6	λ	σ_n	D
j_m	1.0000			−1.0000				
α_m	17.2629			−13.0593		3.285m	6.5cm	25.1
β_m	−0.0552			−3.1484				
j_m	1.0000	−1.0000						
α_m	22.6467	−16.9115				4.309m	31.4cm	6.9
β_m	−1.0227	−3.7125						
j_m	1.0000	4.0000	−5.0000					
α_m	18.5565	55.4284	−71.0930			3.531m	13.3cm	13.3
β_m	−0.2342	−0.8502	−0.8075					
j_m	1.0000			1.0000	−2.0000			
α_m	21.1223			15.9789	−34.2894	4.019m	5.1cm	39.2
β_m	−0.0200			−1.1422	−0.6495			
j_m	1.0000	1.0000	0.0000		−2.0000			
α_m	23.4845	17.5371	0.0000		−38.1242	4.469m	6.3cm	35.3
β_m	−0.0468	−0.1700	−0.1615		−1.5191			

Table 3 GP-IF-NP mixed code-carrier widelane combinations of max. discrimination for $\sigma_\phi = 2\text{mm}$, $\sigma_{\rho_m} = 3 \cdot \Gamma_m$

	E1	E5a	E5b	E5	E6	λ	σ_n	D
j_m	1.0000			−1.0000				
α_m	17.2629			−13.0593		3.285m	19.0cm	8.6
β_m	−0.0552			−3.1484				
j_m	1.0000	−1.0000						
α_m	22.6467	−16.9115				4.309m	93.8cm	2.3
β_m	−1.0227	−3.7125						
j_m	1.0000	4.0000	−5.0000					
α_m	18.5565	55.4284	−71.0930			3.531m	34.0cm	5.2
β_m	−0.2342	−0.8502	−0.8075					
j_m	1.0000			1.0000	−2.0000			
α_m	21.1223			15.9789	−34.2894	4.019m	11.9cm	16.9
β_m	−0.0200			−1.1422	−0.6495			
j_m	1.0000	1.0000	1.0000		−3.0000			
α_m	22.5147	16.8130	17.2516		−54.8249	4.284m	13.7cm	15.6
β_m	−0.0186	−0.0676	−0.0642		−0.6040			

Table 4 GP-IF-NP mixed code-carrier narrowlane combinations of max. discrimination for $\sigma_\phi = 2\text{mm}$, $\sigma_{\rho_m} = 3 \cdot \Gamma_m$

	E1	E5a	E5b	E5	E6	λ	σ_n	D
j_m	4.0000			−3.0000				
α_m	2.2853			−1.2966		10.87cm	5.3mm	10.3
β_m	0.0002			0.0111				
j_m	4.0000	−3.0000						
α_m	2.2870	−1.2809				10.88cm	5.4mm	10.1
β_m	−0.0013	−0.0048						
j_m	4.0000	−2.0000	−1.0000					
α_m	2.2853	−0.8533	−0.4378			10.87cm	5.0mm	10.8
β_m	0.0007	0.0026	0.0025					
j_m	4.0000			−3.0000	0.0000			
α_m	2.2841			−1.2959	0.0000	10.87cm	5.3mm	10.3
β_m	0.0001			0.0075	0.0042			
j_m	4.0000	−2.0000	−1.0000		0.0000			
α_m	2.2844	−0.8529	−0.4376		0.0000	10.87cm	5.0mm	10.9
β_m	0.0002	0.0006	0.0005		0.0049			

FLATTENING OF AMBIGUITY SPECTRUM WITH MIXED CODE-CARRIER COMBINATIONS

Integer ambiguity resolution within a few seconds is challenging as the negligible change in geometry results in an ill-conditioned system of equations. The standard deviations of conditional ambiguity estimates represent the spectrum of ambiguities and are characterized by a jump of several orders of magnitude between the first and last ambiguity. There exist two approaches to flatten the ambiguity spectrum and thereby reduce the probability of wrong fixing. The first one is integer decorrelation which has been proposed by Teunissen in the LAMBDA method [1]. The integer decorrelation matrix is computed iteratively as

$$\boldsymbol{Z} = \boldsymbol{Z}^{(1)} \cdot \boldsymbol{Z}^{(2)} \cdot \ldots \cdot \boldsymbol{Z}^{(N_{\mathrm{it}})}, \qquad (14)$$

where each $\boldsymbol{Z}^{(n)}$ represents an integer approximated Gaussian elimination and a permutation of ambiguities.

Fig. 1 shows that both the wavelength of the mixed code-carrier combination and the number of chosen decorrelation steps N_{it} have a substantial impact on the probability of wrong fixing. A complete integer decorrelation is optimum due to the absence of biases.

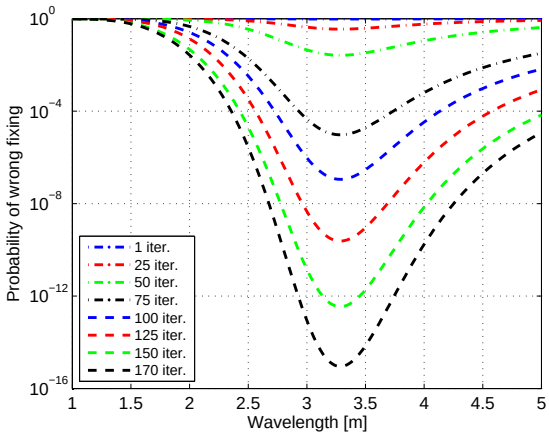

Fig. 1 Benefit of integer decorrelation for ambiguity fixing using an E1-E5 mixed code-carrier combination

The success rate is lower bounded by the success rate of Blewitt's bootstrapping [6]. It is given by Teunissen in [7] as

$$P_{\mathrm{s}} = \prod_{j=1}^{K-1} \left[\Phi\left(\frac{1}{2\sigma_{\hat{N}_{j|\mathfrak{j}}}} \right) + \Phi\left(\frac{1}{2\sigma_{\hat{N}_{j|\mathfrak{j}}}} \right) - 1 \right], \qquad (15)$$

with the cumulative Gaussian distribution

$$\Phi(x) = \int_{-\infty}^{x} \frac{1}{\sqrt{2\pi}} e^{-\frac{1}{2}v^2} dv, \qquad (16)$$

and the conditional ambiguity standard deviation $\sigma_{\hat{N}_{j|\mathfrak{j}}}$. A simulated Galileo geometry over 100 epochs with 11 visible satellites has been assumed. Note that the combination of maximum discrimination also minimizes the probability of wrong fixing for any other geometry.

The second approach to flatten the ambiguity spectrum is the choice of two GP-IF linear combinations: A mixed code-carrier combination of maximum discrimination and an additional code-only combination of minimum noise. The latter one does not introduce any additional ambiguities. It has been shown by the authors in [8] that both combinations are uncorrelated. An almost flat ambiguity spectrum is obtained within a single iteration in Fig. 2. Besides the lower number of decorrelation steps, the two GP-IF linear combinations reduce the spectrum of ambiguities by one order of magnitude compared to the flattened spectrum of a single linear combination of maximum discrimination. The flattening of the spectrum improves the search efficiency and reduces the probability of wrong fixing for bootstrapping substantially.

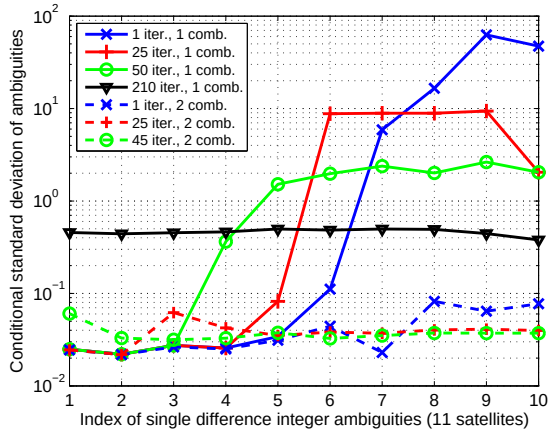

Fig. 2 Spectrum of E1-E5 widelane ambiguities for measurements over 10s: Flattening of the spectrum of the mixed code-carrier combination by an additional code-only combination

PARTIAL INTEGER DECORRELATION FOR BIASED PHASE AND CODE MEASUREMENTS

The LAMBDA algorithm achieves the integer least-square solution for unbiased measurements. However, LAMBDA does not necessarily generate the integer least-square solution for biased measurements as the integer decorrelation amplifies the biases which partially compensates the gain obtained from the variance reduction. Reliable ambiguity resolution is even prevented if the biases are amplified to more than half a cycle. Therefore, partial integer decorrelation is suggested to achieve the optimum trade-off between variance reduction and bias amplification. The partial integer decorrelation is implemented by a reduced number of decorrelation steps, i.e. $N_{\mathrm{it}} < N_{\mathrm{it,max}}$. An additional ionosphere-free carrier smoothing of Hwang et al.

[9] is applied to both linear combinations to reduce the variances which increases the margins for the biases. Fig. 3 and 4 show the probability of wrong fixing as a function of the upper bound on E1 and E5 phase biases for $0°$ elevation and different numbers of integer decorrelation steps. A single step achieves a probability of wrong fixing that is up to 20 orders of magnitude lower than in the case of complete integer decorrelation for phase biases of only 0.05 cycles. An exponential bias profile is assumed where the pendant factor ζ is chosen in both figures such that $b_{\rho,\max}(90°) = 1$ cm. The smoothing period has been set to $\tau = 30$s for both

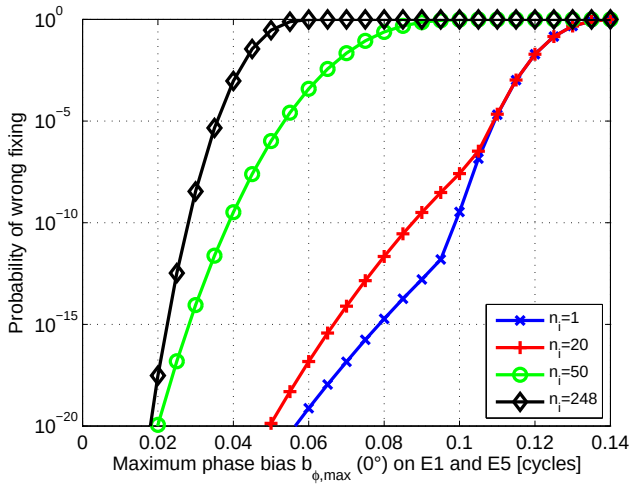

Fig. 3 Probability of wrong fixing of E1-E5 widelane ambiguities for an exponential bias profile ($b_{\rho,\max}(0°) = 2$cm) and a reduced number of integer decorrelation iterations

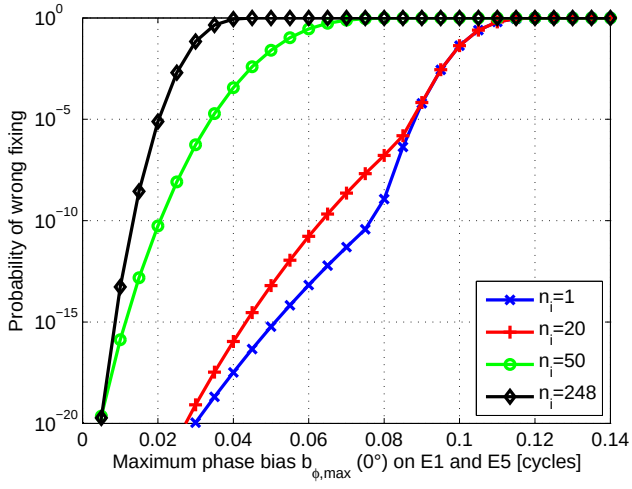

Fig. 4 Probability of wrong fixing of E1-E5 widelane ambiguities for an exponential bias profile ($b_{\rho,\max}(0°) = 5$cm) and a reduced number of integer decorrelation iterations

the mixed code-carrier combination of maximum discrimination (Tab. 3) and the E1-E5 code-only combination of minimum noise.

PARTIAL AMBIGUITY FIXING IN THE PRESENCE OF BIASES

The probability of wrong fixing exceeds 10^{-9} for $b_{\phi,\max}(0°) \geq 0.1$ cycles in Fig. 3 and for $b_{\phi,\max}(0°) \geq 0.08$ cycles in Fig. 4. However, a subset of ambiguities can be fixed reliably for even larger biases.

Bounding of conditional ambiguity biases

The number of fixable ambiguities depends on the chosen subset of ambiguities and the order of fixings within the subset. The optimum subset and fixing order are determined for an upper bound on the conditional ambiguity biases. Teunissen has shown in [7] that the conditional ambiguity biases can be related linearly to the measurement biases for bootstrapping, i.e.

$$\begin{aligned} b_{\hat{N}_{k|\boldsymbol{k}}} \;=\; & \sum_{j=1}^{K-1} \boldsymbol{S}_{kj}\alpha_1\lambda_1 \cdot b_{\phi^j_{\mathrm{E1}}} + \sum_{j=1}^{K-1} \boldsymbol{S}_{kj}\alpha_2\lambda_2 \cdot b_{\phi^j_{\mathrm{E5}}} \\ & + \sum_{j=1}^{K-1} \left(\boldsymbol{S}_{kj}\beta_1 + \boldsymbol{S}_{k,j+(K-1)}b_1\right) \cdot b_{\rho^j_{\mathrm{E1}}} \\ & + \sum_{j=1}^{K-1} \left(\boldsymbol{S}_{kj}\beta_2 + \boldsymbol{S}_{k,j+(K-1)}b_2\right) \cdot b_{\rho^j_{\mathrm{E5}}}, \quad (17) \end{aligned}$$

with the phase weighting coefficients α_1, α_2 and code weighting coefficients β_1, β_2 for the first linear combination, the code weighting coefficients b_1, b_2 for the second linear combination, and

$$\boldsymbol{S} = (\boldsymbol{L}^T)^{-1}\boldsymbol{Z}^T\boldsymbol{P}\left(\boldsymbol{X}^T\boldsymbol{\Sigma}^{-1}\boldsymbol{X}\right)^{-1}\boldsymbol{X}^T\boldsymbol{\Sigma}^{-1}, \quad (18)$$

where $\boldsymbol{L}$ is obtained by Teunissen in [7] from the triangular decomposition of the float ambiguity covariance matrix $\boldsymbol{\Sigma}_{\hat{N}} = \boldsymbol{L}\boldsymbol{D}\boldsymbol{L}^T$. $\boldsymbol{P} = [\boldsymbol{0}^{(K-1)\times 4}, \boldsymbol{1}^{(K-1)\times(K-1)}]$ selects the float ambiguities from the least-square estimate $[\hat{\boldsymbol{x}}, \hat{T}_z, \hat{\boldsymbol{N}}]$ and $\boldsymbol{X}$ relates the two linear combinations of measurements to the unknown parameters $\boldsymbol{x}$, T_z and $\boldsymbol{N}$, i.e.

$$\boldsymbol{X} = \begin{bmatrix} \Delta\boldsymbol{e}^{(1),T} & \Delta m_{\mathrm{w}}^{(1)} & \lambda & & \\ \vdots & \vdots & & \ddots & \\ \Delta\boldsymbol{e}^{(K-1),T} & \Delta m_{\mathrm{w}}^{(K-1)} & & & \lambda \\ \Delta\boldsymbol{e}^{(1),T} & \Delta m_{\mathrm{w}}^{(1)} & 0 & \cdots & 0 \\ \vdots & \vdots & \vdots & \ddots & \vdots \\ \Delta\boldsymbol{e}^{(K-1),T} & \Delta m_{\mathrm{w}}^{(K-1)} & 0 & \cdots & 0 \end{bmatrix}. \quad (19)$$

Equations (17) and (18) show that the conditional ambiguity biases depend on $\boldsymbol{Z}$. Upper bounds on these biases can

be derived from upper bounds on the measurement biases by assuming that all bias terms in (17) accumulate positively, i.e.

$$\begin{aligned} b_{\phi^j_{\mathrm{E1}}} &= \mathrm{sign}\left(\boldsymbol{S}_{kj}\alpha_1\lambda_1\right)\cdot b_{\phi^j_{\mathrm{E1,max}}} \\ b_{\phi^j_{\mathrm{E5}}} &= \mathrm{sign}\left(\boldsymbol{S}_{kj}\alpha_2\lambda_2\right)\cdot b_{\phi^j_{\mathrm{E5,max}}} \\ b_{\rho^j_{\mathrm{E1}}} &= \mathrm{sign}\left(\boldsymbol{S}_{kj}\beta_1 + \boldsymbol{S}_{k,j+(K-1)}b_1\right)\cdot b_{\rho^j_{\mathrm{E1,max}}} \\ b_{\rho^j_{\mathrm{E5}}} &= \mathrm{sign}\left(\boldsymbol{S}_{kj}\beta_2 + \boldsymbol{S}_{k,j+(K-1)}b_2\right)\cdot b_{\rho^j_{\mathrm{E5,max}}}. \end{aligned} \tag{20}$$

An exponential profile is chosen for both phase and code biases on E1 and E5, i.e.

$$\begin{aligned} b_{\phi^j_{\mathrm{E1,max}}} &= b_{\phi_{\mathrm{E1,max}}}(\theta=0^\circ)\cdot e^{-\theta^{(j)}/\zeta_{\phi_{\mathrm{E1}}}} \\ b_{\phi^j_{\mathrm{E5,max}}} &= b_{\phi_{\mathrm{E5,max}}}(\theta=0^\circ)\cdot e^{-\theta^{(j)}/\zeta_{\phi_{\mathrm{E5}}}} \\ b_{\rho^j_{\mathrm{E1,max}}} &= b_{\rho_{\mathrm{E1,max}}}(\theta=0^\circ)\cdot e^{-\theta^{(j)}/\zeta_{\rho_{\mathrm{E1}}}} \\ b_{\rho^j_{\mathrm{E5,max}}} &= b_{\rho_{\mathrm{E5,max}}}(\theta=0^\circ)\cdot e^{-\theta^{(j)}/\zeta_{\rho_{\mathrm{E5}}}}, \end{aligned} \tag{21}$$

with the decay constants $\zeta_{\phi_{\mathrm{E1}}}$, $\zeta_{\phi_{\mathrm{E5}}}$, $\zeta_{\rho_{\mathrm{E1}}}$, $\zeta_{\rho_{\mathrm{E5}}}$ and elevation angle θ. Table 5 depicts the chosen parameters for the exponential profiles.

Table 5 Parameters of exponential bias profile

	$b_{\phi_{\mathrm{E1,max}}}$	$b_{\phi_{\mathrm{E5,max}}}$	$b_{\rho_{\mathrm{E1,max}}}$	$b_{\rho_{\mathrm{E5,max}}}$
$\theta = 0^\circ$	0.1 cyc.	0.1 cyc.	10 cm	10 cm
$\theta = 90^\circ$	0.01 cyc.	0.01 cyc.	1 cm	1 cm

Fig. 5 shows the conditional ambiguity biases $b_{\hat{N}_{k|\boldsymbol{k}}}$ that have been computed from (17)-(21) for a snapshot of simulated Galileo measurements. Two orders of ambiguity fixings are considered: The first one is chosen to maximize the number of reliably fixable ambiguities N_p while the second one is based on the PRN and suffers from a large bias for the first ambiguity to be fixed. A 30 s carrier smoothing is performed and no integer decorrelation is applied to avoid bias amplification. The success rate of bootstrapping for biased measurements has been derived by Teunissen in [7] and is given by

$$P_{\mathrm{s}} = \prod_{j=1}^{K-1}\left[\Phi\left(\frac{1-2b_{\hat{N}_{j|\boldsymbol{j}}}}{2\sigma_{\hat{N}_{j|\boldsymbol{j}}}}\right)+\Phi\left(\frac{1+2b_{\hat{N}_{j|\boldsymbol{j}}}}{2\sigma_{\hat{N}_{j|\boldsymbol{j}}}}\right)-1\right], \tag{22}$$

with the cumulative Gaussian distribution of (16). Fig. 6 shows the achievable probability of wrong fixing for the bias bounds of Fig. 5. $N_p = 5$ ambiguities can be fixed with a probability of wrong fixing of less than 10^{-9} for an optimized order while no ambiguities can be fixed when the order is taken from the PRNs.

Search tree for optimum fixing order determination

There exist $(K-1)!$ orders of single difference ambiguity fixings for K visible satellites. These fixing orders can

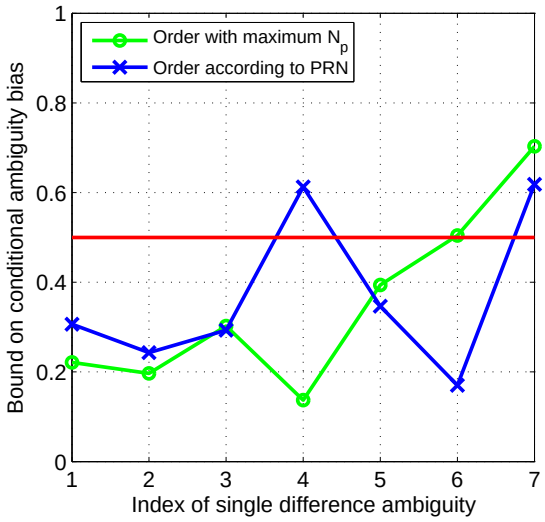

Fig. 5 Bound on conditional ambiguity biases using two carrier smoothed E1-E5 GP-IF combinations (code-carrier combination of max. discrimination, code-only combination of minimum noise) for an exponential bias profile for both code and carrier phase on E1 and E5

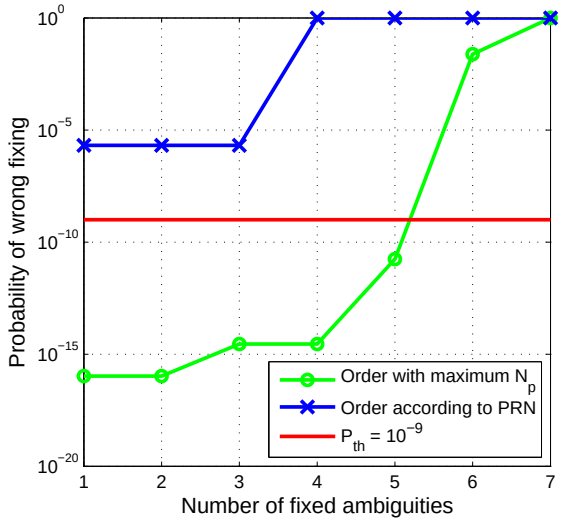

Fig. 6 Probability of wrong ambiguity fixings using two carrier smoothed E1-E5 GP-IF combinations (code-carrier combination of max. discrimination, code-only combination of minimum noise) for an exponential bias profile for both code and carrier phase on E1 and E5

be represented by $K-1$ trees where each node refers to an ambiguity and each branch is characterized by a probability of wrong fixing. Obviously, an exhaustive search of the optimum order is often unfeasible. However, the sequential construction of the trees from the root with two constraints allows a dramatic reduction of the search space. First, the probability of wrong fixing is computed for each node and

once it exceeds the threshold of 10^{-9} this branch is no longer extended. Secondly, a low probability of wrong fixing requires good satellite geometry which motivates a minimum azimuthal separation between two consecutively fixed ambiguities. Fig. 7 shows an exemplary skyplot where the number of fixing candidates is reduced from 10 to 7 in the first fixing step. The requirement of azimuthal separation is weakened with the increase of fixed ambiguities to enable a fixing of the few remaining ambiguities, i.e.

$$|\mathrm{azi}^{(k)} - \mathrm{azi}^{(k+1)}| \overset{!}{>} \frac{K-1-k}{K-2} \cdot \Delta\mathrm{azi}_{\max}, \qquad (23)$$

where $\Delta\mathrm{azi}_{\max}$ denotes the azimuthal requirement between the first two fixings.

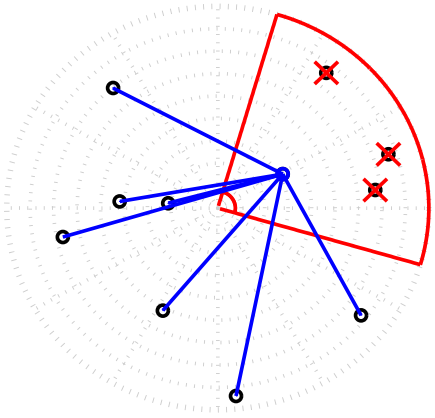

Fig. 7 Skyplot with azimuthal separation requirement to reduce the search space of fixing orders

The two requirements simplify the search tree in different ways, i.e. the first requirement is stringent for long branches while the second requirement is more strict for shorter branches. The choice of $\Delta\mathrm{azi}_{\max}$ is a trade-off between a reduction of the search space and a decrease in fixable ambiguities. Fig. 8 shows the maximum number of fixable ambiguities for $\Delta\mathrm{azi}_{\max} = 45°$ and a simulated Galileo geometry at $48.1507°$ latitude and $11.569°$ longitude. At least four ambiguities can be fixed reliably at any time for the optimized sorting which is a substantial improvement over the PRN based sorting. The exponential bias profile of Table 5 and a 30 s smoothing period have been chosen.

Fig. 9 shows the number of tree branches for azimuthal constraint partial ambiguity fixing with $\Delta\mathrm{azi}_{\max} = 45°$. A maximum of a few thousand branches is obtained which is several orders of magnitude lower than the $(K-1)!$ possible branches of length $K-1$. It is recommended to adapt the azimuthal separation constraint to the number of visible satellites, i.e. to choose a larger $\Delta\mathrm{azi}_{\max}$ if more than 8 satellites are visible.

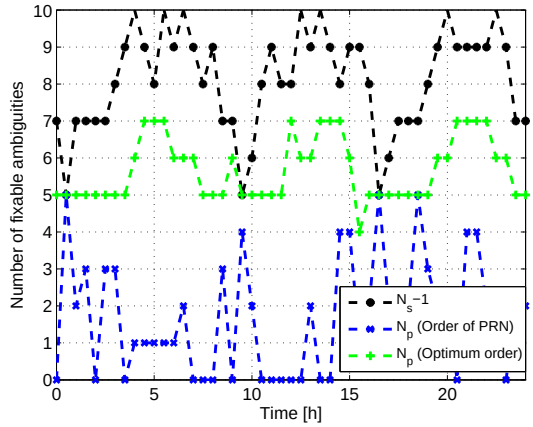

Fig. 8 Number of fixable ambiguities using two carrier smoothed E1-E5 GP-IF combinations (code-carrier combination of max. discrimination, code-only combination of minimum noise) for an exponential bias profile for both code and carrier phase on E1 and E5

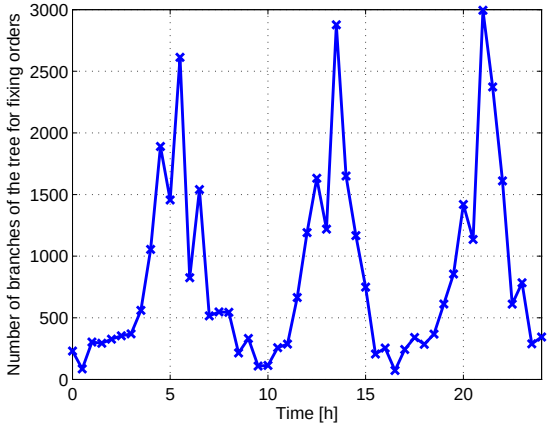

Fig. 9 Number of tree branches for azimuth constraint partial ambiguity fixing orders

Skyplots for optimal fixing strategy

Fig. 10 - 12 show the optimum fixing orders in skyplots for three different geometries and an exponential bias profile. The reference satellite used for all single differences is marked in red and the first satellite to be fixed is marked by a square symbol. The azimuthal separation constraint leads to fast covering of the complete sky within a few fixes whereas the satellites of lowest elevation are not included due to severe biases. The choice of the optimum order enables the fixing of a significantly larger number of ambiguities than for the PRN based order, e.g. 7 single difference am-

biguities are fixable instead of a single one in Fig. 12.

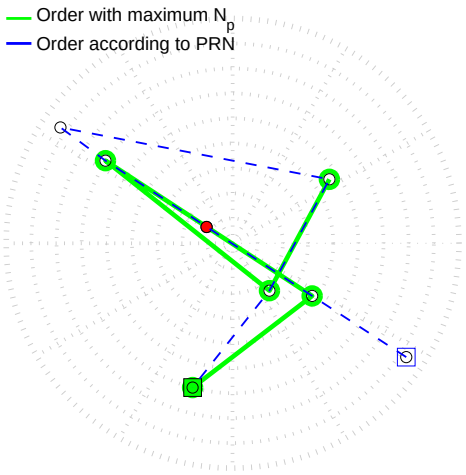

Fig. 10 Skyplot for azimuth constraint partial ambiguity fixing with $\tau = 30s$ smoothing and an exponential bias profile for both code and carrier phase on E1 and E5

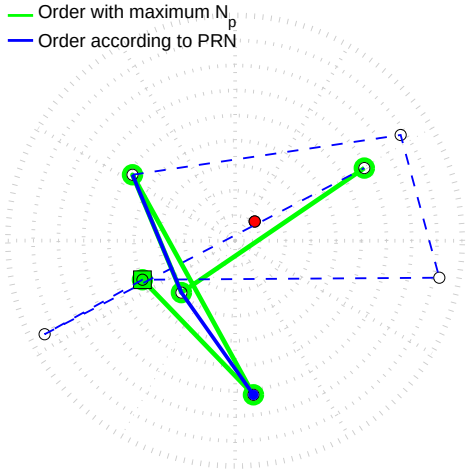

Fig. 11 Skyplot for azimuth constraint partial ambiguity fixing with $\tau = 30s$ smoothing and an exponential bias profile for both code and carrier phase on E1 and E5

Maximum number of fixable ambiguities

The number of fixable ambiguities N_p decreases for severe carrier phase multipath which results in phase biases up to $\lambda/4$ if the line of sight signal is not shadowed. Fig. 13 shows N_p as a function of the maximum phase bias $b_{\phi_{\max}}(0°)$ (for both E1 and E5) for a snapshot of simulated Galileo measurements. The tree of fixing orders has been generated again sequentially using the constraints on

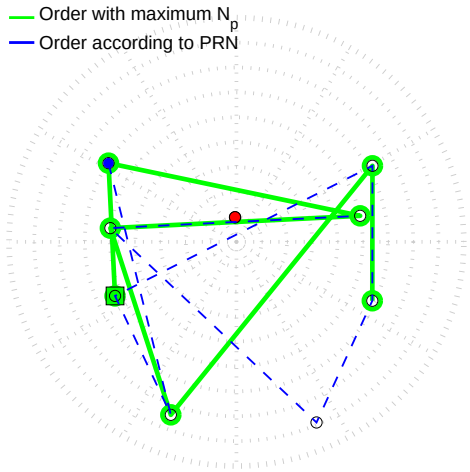

Fig. 12 Skyplot for azimuth constraint partial ambiguity fixing with $\tau = 30s$ smoothing and an exponential bias profile for both code and carrier phase on E1 and E5

the probability of wrong fixing (10^{-9}) and the azimuthal separation ($45°$).

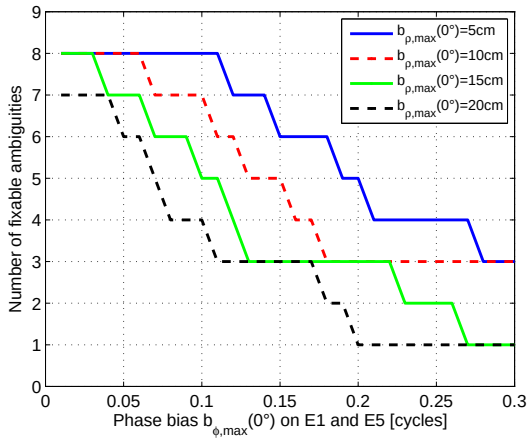

Fig. 13 Number of fixable ambiguities for azimuth constraint optimum fixing order, $\tau = 30s$ smoothing and an exponential bias profile for both code and carrier phase on E1 and E5

Fig. 14 shows the impact of the carrier smoothing time τ on the number of fixable ambiguities. For large smoothing periods, N_p converges to the number of conditional ambiguity biases that are smaller than 0.5. The proposed partial ambiguity fixing scheme is rather insensitive w.r.t. the satellite geometry, which is not the case for LAMBDA with complete integer decorrelation. Fig. 15 shows that at least four ambiguities can be fixed with a probability of wrong fixing of 10^{-9} through Europe for a selected snapshot with the previous bias bounds.

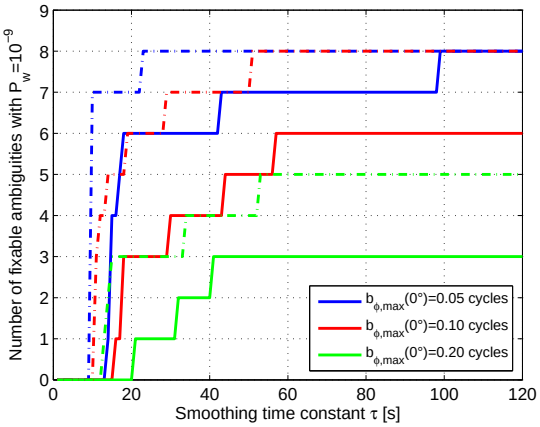

Fig. 14 Impact of carrier smoothing time τ on partial ambiguity fixing for an exponential bias profile

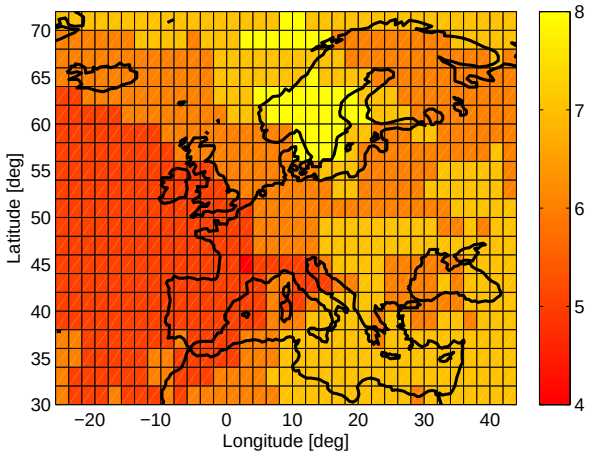

Fig. 15 Number of fixable ambiguities with a probability of wrong fixing of 10^{-9} for two carrier smoothed GP-IF linear combinations (code-carrier combination of max. discrimination, code-only combination of minimum noise) and an exponential bias profile

CONCLUSIONS

In this paper, ionosphere-free mixed code-carrier combinations with two, three and four Galileo frequencies have been derived. The noisy code measurements are only used with a small weight but help significantly to obtain a linear combination that eliminates the ionosphere and preserves the integer nature of ambiguities. An E1-E5a-E5b-E6 combination with a wavelength of 4.469 m and a noise level of a few centimeters was found. It suppresses the E1 code noise and multipath by 13.3 dB which increases effectively to 27.0 dB when the wavelength scaling is taken into account. The integer ambiguity resolution is generally performed by LAMBDA which achieves the integer least-square solution for unbiased measurements. For biased measurements, the LAMBDA decorrelation transformation amplifies the biases substantially which prevents an integer least-square solution. Therefore, a partial integer decorrelation has been suggested to achieve the optimum trade-off between variance reduction and bias amplification. The probability of wrong fixing can be reduced by several orders of magnitude compared to a complete integer decorrelation for phase biases of only 0.05 cycles. For larger biases, partial ambiguity fixing was analyzed with a new efficient method for the search of the largest subset of reliably fixable ambiguities. Constraints on the probability of wrong fixing and the azimuthal separation between two consecutively fixed ambiguities allow a substantial reduction of the number of possible fixing orders. The optimum order has been shown for an exponential bias profile in skyplots.

REFERENCES

[1] P. Teunissen, *Least-squares estimation of the integer ambiguities*, Invited lecture, Section IV, Theory and Methodology, IAG General Meeting, Beijing, China, 1993.

[2] P. de Jonge and C. Tiberius, *The LAMBDA method for integer ambiguity estimation: implementation aspects*, Publications of the Delft Geodetic Computing Centre, no. 12, Aug. 1996.

[3] H. Euler and B. Schaffrin, *On a Measure for the Discernibility Between Different Ambiguity Solutions in the StaticKinematic GPS-Mode*, IAG Symposia no. 107, Kinematic Systems in Geodesy, Surveying, and Remote Sensing, Springer-Verlag, New York, pp. 285 295, 1991.

[4] P. Henkel and C. Günther, *Joint L/C-Band Code-Carrier Linear Combinations for Galileo*, International Journal of Navigation and Observation, Special Issue on Future GNSS Signals, Hindawi Publ., Jan. 2008.

[5] J. Betz, *Binary Offset Carrier Modulations for Radionavigation*, Navigation, Vol. 48, No. 4, pp. 227-246, 2002.

[6] G. Blewitt, *Carrier-phase ambiguity resolution for the Global Positioning System applied to geodetic baselines up to 2000 km*, Journal Geophysic Research, Vol. 94, pp. 10187-10203, 1989.

[7] P. Teunissen, *Integer estimation in the presence of biases*, Journal of Geodesy, pp. 399-407, Springer, 2001.

[8] P. Henkel and C. Günther, *Precise Point Positioning with multiple Galileo frequencies*, Proc. of the Positioning, Location and Navigation Symposium (PLANS), Monterey, USA, pp. 592-599, May 2008.

[9] P. Hwang, G. Graw and J. Bader, *Enhanced Differential GPS Carrier-Smoothed Code Processing Using Dual-Frequency Measurements*, J. of Navigation, vol. 46, No. 2, pp. 127-137, Summer 1999.